BEAM DYNAMICS VERIFICATION IN LINACS OF LINEAR COLLIDERS*

JOHN T. SEEMAN

Stanford Linear Accelerator Center, Stanford University, Stanford, CA 94309

ABSTRACT

The SLAC two-mile linac has been upgraded to accelerate high current, low emittance electron and positron beams to be used in the SLAC Linear Collider (SLC). After the upgrade was completed, extensive beam studies were made to verify that the design criteria have been met. These tests involved the measurement of emittance, beam phase space orientation, energy dispersion, trajectory oscillations, bunch length, energy spectrum and wakefields. The methods, the systems and the data cross checks are compared for the various measurements. Implications for the next linear collider are discussed.

INTRODUCTION

An important requirement of the linac of the SLC is to maintain the low emittance, small energy spectrum, bunch length and intensity of each of the bunches in the beam as they are accelerated from 1.2 to 50 GeV. Once that statement is accepted, a collection of instrumentation packages and a sequence of accelerator experiments are needed to adjust the beams into specification and to verify that these conditions are met. Descriptions of the SLC linac requirements are given in several reports[1,2,3] which are summarized in Table 1. The parameters have ranges because the machine must operate in several configurations depending on the beam intensity, tune up conditions and experimental data taking. The conditions listed here are not unlike a "preinjector" for a large linear collider except that the beam emittances will be lower by at least an order of magnitude.

Table 1. SLAC linac parameters at 50 GeV.

Parameter	Symbol	Range
Rate	f	120 Hz
Bunch Length	σ_z	0.5 to 1.5 mm
Bunch Intensity	$N^{+,-}$	0.1 to 7.2 $\times 10^{10}$
Energy Spectrum	σ_E/E	0.2 to 0.3%
Invariant Emittance	$\gamma\epsilon$	3.0 to 3.5 $\times 10^{-5}$r-m
Energy Gain	E	40 to 55 GeV
Lattice Mismatch	$\triangle\beta$	Less than 10%
Stability (position)	$\triangle x(y)$	$\triangle x(y) \leq 0.5\sigma_{x(y)}$
Stability (energy)	$\triangle E/E$	Less than 0.1%
Lattice	β_{max}	10 to 60 m

* Work supported by the Department of Energy, contract DE-AC03-76SF00515.

BUNCH LENGTH COMPRESSION

The bunch length of the beam exiting the damping ring is about 6 mm which must be shortened to about 0.5 to 1.5 mm before entering the linac. The compression is performed by adding a longitudinal position–energy correlation in the beam using an RF accelerator run at a phase of 90°.[4] A schematic layout is shown in Fig. 1. The dispersion function in the Ring-to-Linac (RTL) transport line is tailored to bring the head and tail particles to the center of the bunch. The resulting minimum bunch length is given by the natural energy spectrum of the damping ring beam. In the center of the transport line the horizontal dispersion is about 1.3 m. With a spectrum of about 0.9% the beam width σ_{xE} due to energy is 25 mm, which is much larger than the betatron size of the beam ($\sigma_{x\beta}$ = 0.5 mm). The dispersion function η must be cancelled to about 1 mm at the entrance to the linac so that the effective emittance of the beam does not enlarge. If an anomalous dispersion does enter the linac, filamentation of the phase space in the chromatic linac lattice will result in an increased beam emittance.

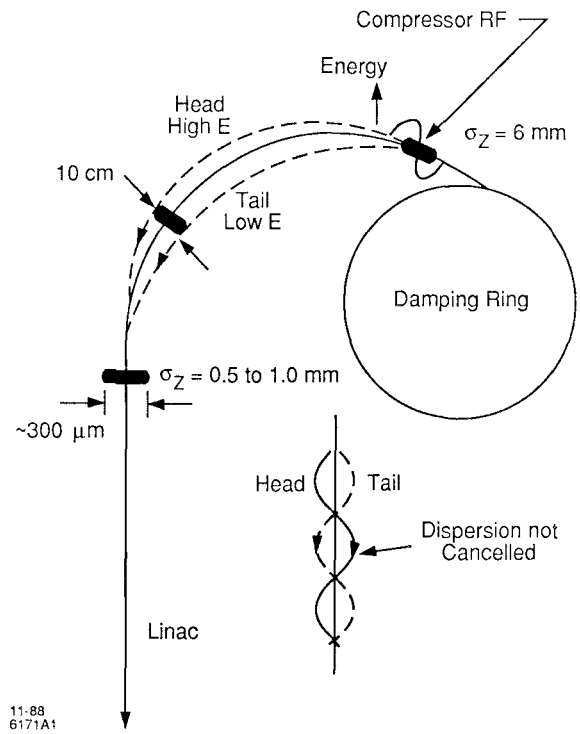

Fig. 1. After exiting the damping ring, each bunch is longitudinally compressed in the RTL transport line using an RF accelerator or compressor. The beam energy is 1.15 GeV, and the RF compressor provides a maximum of 32 MeV acceleration. The bunch center passes at the RF zero crossing. The energy dispersion η in the RTL must be cancelled to about one millimeter as the beam enters the Linac or else there will be anomalous dispersion which will enlarge the effective beam emittance.

The increased emittance ϵ can be calculated given the energy spectrum δ, the anomalous dispersion functions η, η', the nominal emittance ϵ_o and the nominal TWISS parameters β, α and γ:

$$\epsilon = \epsilon_o \left[1 + \frac{\delta^2[\beta\eta'^2 + \gamma\eta^2 + 2\eta\eta'\alpha]}{\epsilon_o}\right]^{\frac{1}{2}} \quad . \tag{1}$$

DISPERSION CORRECTION AT THE LINAC ENTRANCE

The dispersion can be corrected by measuring the anomalous dispersion functions η and η' in the linac and adjusting quadrupoles in the RTL. The measurements involve changing the energy of the beam by changing the phase of the RF compressor and observing transverse beam motion in the linac. The beam movements are measured with strip line beam position monitors[5] with accuracies of order 10 μ in differential motions:

$$\eta = \triangle x E_o / E_c \sin \triangle\phi_c \quad , \tag{2}$$

where $\triangle x$ is the beam motion, E_o the nominal beam energy, E_c the compressor maximum acceleration, and $\triangle\phi_c$ the phase change of the compressor.

Typical measurements of the dispersion are shown in Fig. 2. Results in Fig. 2(a) were made without correction showing dispersions up to 20 mm. With slight changes of the RTL quadrupoles it was possible to minimize the dispersion as in Fig. 2(b) without affecting the beta function. However, when the emittance of the beam was measured after correction in the early part of the linac, it was found to be larger than before. Alternatively, if the dispersion correction was done by minimizing the measured emittance rather than the measured dispersion, the emittance could in fact be reduced to near the design values.

The question which remained was why the direct dispersion correction was incorrect. The answer lies in transverse deflections in the RF compressor. RF deflections[6] are present in all accelerators at some level and are corrected in the steady state by static dipole adjustments. When the phase of the compressor was changed during the dispersion measurements, its deflection also changed, and a betatron oscillation was generated. (See Fig. 3.) The oscillation introduced during a dispersion measurement can be calculated given the maximum RF deflection θ_m:

$$\begin{aligned} x(s) = \theta_m[\sin(\phi_{c1} - \phi_o) \; - \sin(\phi_{c2} - \phi_o)] \\ [\beta_c\beta(s)]^{\frac{1}{2}} \; \sin\,(\psi(s) - \psi_c) \quad , \end{aligned} \tag{3}$$

where ϕ_{c1} and ϕ_{c2} are the two compressor phase settings during the dispersion measurement, ϕ_o the compressor setting corresponding with the maximum deflection, β_c and $\beta(s)$ are the TWISS functions at the compressor and at a longitudinal position s, and $\psi(s)$ and ψ_c are the betatron phases at position s and the compressor, respectively.

The effect on the position of the beam in the linac due to the dispersion generated by the correction quadrupoles in the RTL can be written in a form similar to Eq. (3):

$$x(s) = \frac{E_c}{E_o}[\sin(\phi_{c1}) - \sin(\phi_{c2})]\triangle\eta \sin(\psi(s) - \psi_\eta) \quad , \tag{4}$$

where $\triangle\eta$ is the amplitude of the induced dispersion, and ψ_η is the effective betatron phase at the RTL quadrupoles. Clearly, the position change from deflection changes (Eq. 3) can be corrected by the dispersion adjustment (Eq. 4) by setting $\psi_\eta = \psi_c + n2\pi$ and setting $\triangle\eta$ so that the coefficients are equal.

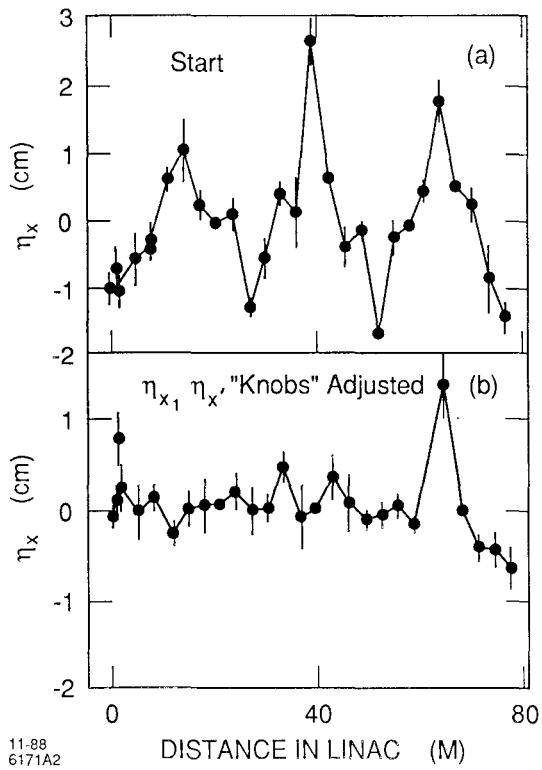

Fig. 2. The anomalous dispersion from the RTL transport line can be measured by changing the compressor phase which changes the beam energy and the trajectory in the linac (a). With the use of quadrupole combinations in the RTL (i.e., η and $\eta\prime$ adjustments), the apparent dispersion can be minimized ($\leq$ 1 mm) (b). However, after this procedure, it was shown not to minimize the measured effective beam emittance. (See Fig. 3).

Thus, the dispersion adjustments cannot distinguish between RF deflection changes and actual dispersion and produce incorrect solutions when the deflections become large. The required RF deflection θ_m, which can explain the data in Fig. 2, is 32 μrad or [37 KeV/1150 MeV]. There are several mechanisms which can produce this deflection.[6]

BUNCH LENGTH MEASUREMENTS

The length of the bunch in the SLC linac after compression in the RTL transport line is in the range of 0.5 to 1.5 mm. The shorter the bunch is, the more difficult the longitudinal wakefields are. The longer the bunch the transverse wakes are more difficult. A compromise is needed in order to manage the growth of the transverse beam size, to maintain a small energy spectrum and to provide enough acceleration.

A system to measure the longitudinal profile of the bunch is shown in Fig. 4. The bunch is accelerated from 1.15 GeV to about 15 GeV in the linac and is transported to a spectrometer where the beam is bent horizontally. The transverse profile is measured on a phosphor screen[7] where the horizontal dispersion η_o is about 0.66 m. The profile width is minimized by adjusting the linac overall phase to minimize σ_E/E and by adjusting upstream quadrupoles to minimize the horizontal betatron function at the profile monitor. The minimized profile is then recorded as shown in Fig. 5(a). Then eight klystrons immediately in front of the spectrometer are triggered on the beam but with their phase offset by 90°. In this condition the head and tail of the bunch receive opposite energy changes. As a result, the energy spectrum increases in proportion to the longitudinal length. See Fig. 5(b).

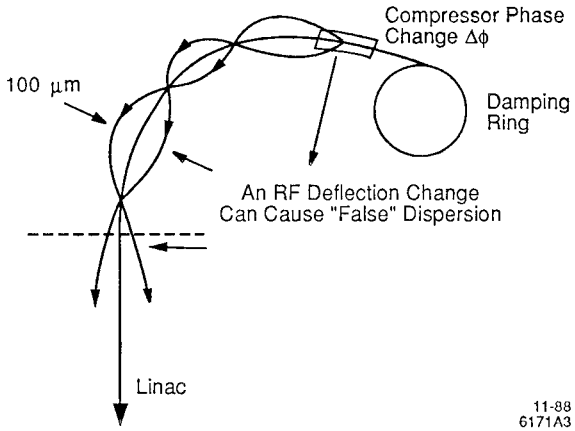

Fig. 3. RF deflections from the compressor can cause head–tail deflection changes during linac dispersion measurements which mimic real dispersion.

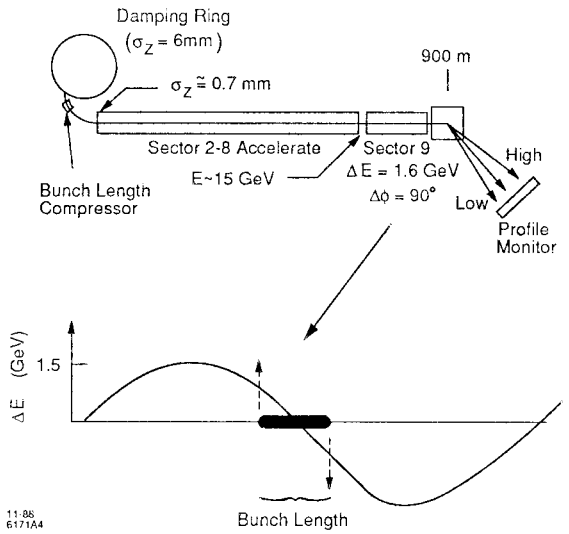

Fig. 4. The bunch length in the linac is measured at 15 GeV by using RF acceleration (1.6 GeV) phased at 90° to expand the energy spectrum depending on the bunch length. The energy spectrum is measured in a spectrometer.

The bunch length σ_z can be calculated from these measurements. Since the bunch length is much shorter than the RF wavelength λ_{RF}, a linear approximation to the sine curve is accurate:

$$\sigma_z = \frac{[\sigma_x^2 - \sigma_{xo}^2]^{\frac{1}{2}} \; E_o \; \lambda_{RF}}{2\pi \; \eta_o \; E_e} \quad , \qquad (5)$$

where σ_x is the beam width with the spectrum expander on; σ_{xo} the width with the expander turned off. E_o is the nominal beam energy (15 GeV); E_e the energy gain of the spectrum expander (1.6 GeV). An example of this method is shown in Fig. 6 where the linac bunch length is measured as as function of beam intensity. A threshold in the bunch length is observed just above $1 \times 10^{10} e^-$ per bunch due to effects in the damping ring.[8]

The resolution of our system is about 60 μ in the bunch length. With effort, this resolution could be reduced and would be sufficient for measuring bunch lengths of order 50 μ envisioned for the next linear collider.

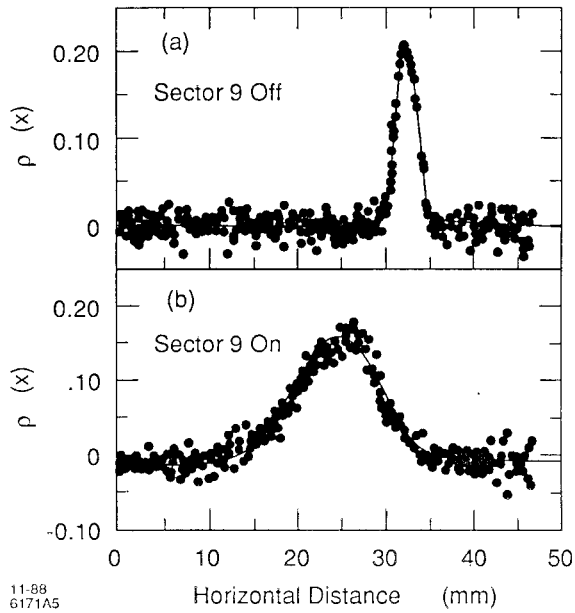

Fig. 5. Typical bunch width measurements with the spectrometer in Fig. 4 when the energy expander was turned off (a) and on (b). The bunch length measured in this example is 0.9 mm.

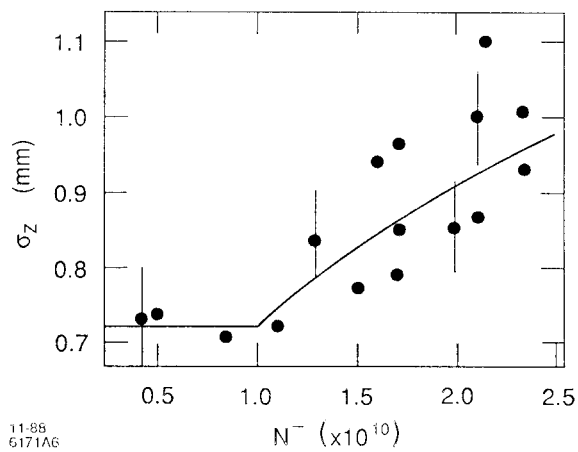

Fig. 6. Bunch length measurements versus N^-.

LATTICE CHECKS

The quadrupoles in the linac keep the beams in focus as they are accelerated. The focusing strengths must match the beam energy at each location in the linac so that a known lattice is maintained. A known lattice allows long range trajectory correction, proper transverse wakefield damping and minimized chromatic beam enlargement.

Errors in the lattice are caused by set point errors in the quadrupoles or by errors in the calculated klystron energy gains. Errors in the quadrupole settings are checked routinely with a "clip-on" ampere meter to verify that the computer data base and the hardware are correct. An occasional problem with the 276 quadrupoles is found and corrected.

The calculated klystron energy gains are determined from calibrated RF amplitude measurements and phase settings. The phase and amplitudes are checked by measuring the beam energy as a function of the klystron phase. Phase settings are measured to about two degrees and acceleration to about 12 MeV out of 225 MeV. The phase and amplitude change slowly with time, and these phase and amplitude measurements must be repeated regularly. Because these measurements are costly of beam time, an alternate approach was developed.

Trajectory oscillations can be used to verify that the energy gains and phases are correct.[9] Several dipoles along the linac are varied to introduce beam oscillations. An on-line model of the linac is used to predict these oscillations. In Fig. 7 are shown two plots where oscillation data and the model predictions are compared. In Fig. 7(a) a mis-phased klystron has produced a mismatch in the energy profile in the linac. The beam has a lower energy than it should, and the oscillations occur more rapidly. In Fig. 7(b) the lattice and the prediction agree very well indicating a proper lattice. There are approximately nine position readings per wavelength.

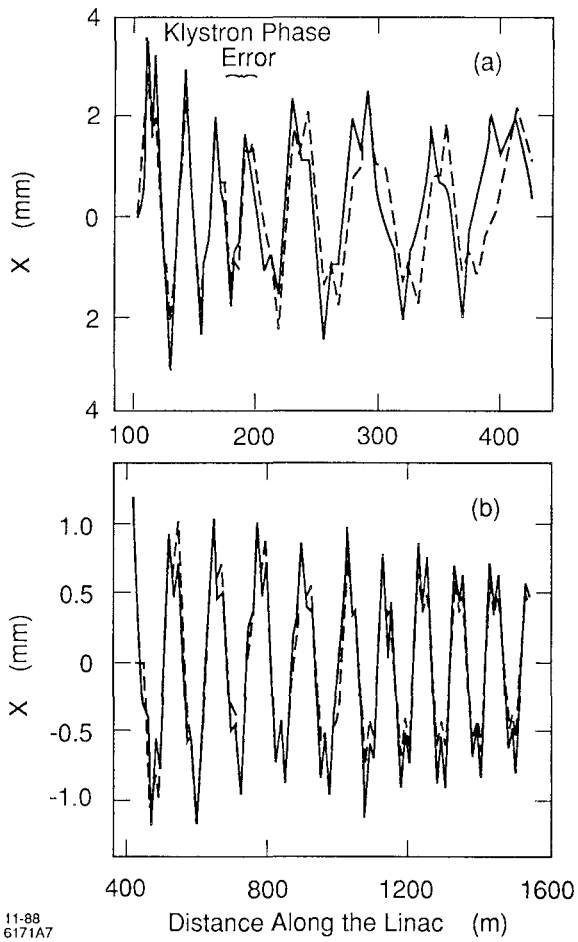

Fig. 7. Induced oscillations in the SLC linac showing the measured trajectory (solid lines) and the predicted trajectory from the online computer model (dashed lines). Differences between the data and prediction indicate errors. A klystron RF phase error is detected in (a) and no errors in (b).

The sensitivity of this method depends on the phase advance per cell. In the SLC linac the quadrupole lattice is very strong in the beginning and becomes much weaker at the end.[2] The angular oscillation frequency ν changes with energy E depending on the value of ν:

$$\frac{d\nu}{\nu} = \frac{-2(1-\cos\nu)}{\nu \sin\nu}\,\frac{dE}{E} \quad . \tag{6}$$

As the value of $\nu/2\pi$ changes from 90^o per cell in the early linac to 45^o at the end, the value of $E/\nu\ d\nu/dE$ changes from -1.27 to -1.06. Thus, a smaller response is expected late in the linac.

The ability of this method to check the lattice is dependent on the fractional energy contribution of each klystron and on how the errors accumulate. The first klystron adds 220 MeV/1150 MeV or 22% to the energy of the beam; the last klystron 220 MeV/47000 MeV or 0.5%. Thus, much larger gain errors must occur in the downstream part of the linac in order for the lattice checks to be sensitive to them.

Finally, the errors in the calibration of the klystron energy gains accumulate statistically along the linac and can be estimated given the initial beam energy E_0, (1.15 GeV), the gain of a typical klystron E_i (200 MeV), and the calibration error $\triangle E$ ($\sim$ 12 MeV). The fractional error f on the total energy is given by

$$f = \frac{\sqrt{n}\ \triangle E}{E_o + nE_i} \quad , \tag{7}$$

where n is the number of klystrons upstream of the position of interest: f varies from 0.009 for $n = 1$, to 0.011 for $n = 10$, and finally, 0.004 for $n = 222$. Therefore, the expected statistical error in the calculated energy is of order 1% through the linac.

ENERGY SPECTRUM MEASUREMENT

The energy spectra of the positron and electron beams are measured near the end of the linac in a known dispersion region at the beginning of the SLC arcs. A schematic view of this measurement is shown in Fig. 8. After the beam has been bent, the beam profile is viewed either on an intercepting monitor[10] or continuously on a non-intercepting X-ray monitor. The profile σ_x is obtained through a digitized TV image. The spectrum is calculated as $\delta = \sigma_x/\eta_o$, where η_o is the nominal dispersion generated by the dipole. The measurements can be taken at 1 Hz. Each spectrum can be independently adjusted by using the respective damping ring phase.

The profile monitor has been placed in a special location where the energy dispersed beam size σ_{xE} dominates the betatron size $\sigma_{x\beta}$:

$$\sigma_x^2 = \sigma_{xE}^2 + \sigma_{x\beta}^2 \quad , \tag{8}$$

where

$$\sigma_{xE} = \eta_o\delta \approx (70\text{ mm})(0.2\%) = 140\ \mu\text{m}$$

and

$$\sigma_{x\beta} = [\beta_o\epsilon_o]^{\frac{1}{2}} \approx [(2\text{ m})(3\times10^{-10}r - \text{m})]^{\frac{1}{2}} = 25\ \mu\text{m} \quad ,$$

and β_o and ϵ are the TWISS parameters at the profile monitor.

Errors in the beam phase space such as anomalous dispersion and betatron mismatches will distort the spectrum measurements. An example of a distortion is shown in Fig. 8 where anomalous dispersion (or energy-position correlation η) in the beam changes the beam's profile depending on the amplitude and phase of the anomalous dispersion.

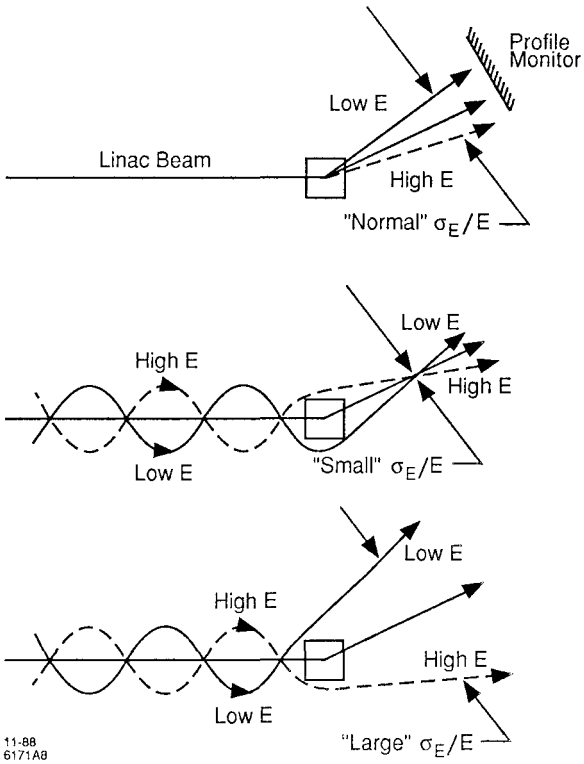

Fig. 8. The energy spectrum of each beam is measured at the end of the linac in a known dispersive region. The spectrum is given by the horizontal width of the beam profile. Anomalous dispersion of the beam in the linac can distort the profile measurement. The measured width depends on the amplitude and phase of the anomalous dispersion.

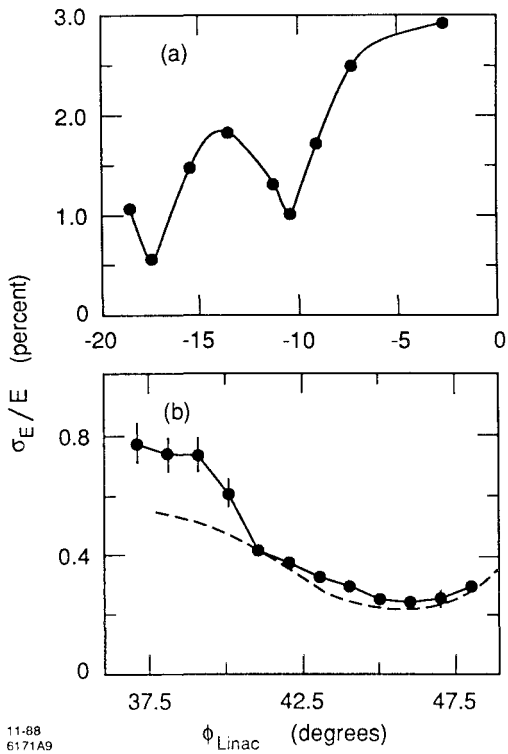

Fig. 9. Measured energy spectra of 47 GeV beams as a function of the linac overall RF phase. The measurement (a) is contaminated by anomalous dispersion in the linac which changes phase with the linac RF phase (because of energy). The measurement (b) has the anomalous dispersion in the linac removed and is close to the theoretical value.

The above phenomena can be written in an equation for the effective spectrum δ_{eff} for small betatron mismatches:

$$\delta_{eff}^2 = \frac{\sigma_x^2}{\eta_o^2} = \frac{1}{\eta_o^2}\left[(\eta_o + \eta\cos\phi_\beta)^2\delta^2\right]$$

$$+\frac{\epsilon_o\beta_o}{\eta_0^2}\left(1+\frac{\Delta\beta}{\beta_0}\cos 2[\phi_\beta+\phi_{\beta_o}]\right) \quad , \qquad (9)$$

where ϕ_β is the betatron phase advance from the source of η, ϕ_{β_o} an arbitrary phase, δ the actual energy spectrum, and $\Delta\beta/\beta_0$ the mismatch of the TWISS parameter of the beam compared to the lattice. Here, δ, ϕ_β, and $\Delta\beta/\beta_0$ change as the overall RF phase is adjusted to minimize δ. Recent estimates or measurments of the variables give $\eta_o = 70$ mm, $\eta \approx 10$ mm, $\delta = 0.25\%$, $\epsilon_o = 6\times10^{-10}r-$m, $\beta_o = 2$m, and $\Delta\beta < 2$ m. With these values only η contributes significantly to the spectrum measurement.

An example of the anomalous dispersion term is shown in Fig. 9. Early in the commissioning of the SLC the anomalous dispersion η was comparable to η_o. As the linac phase was varied the betatron phase advance from the source of the dispersion (unknown in practice as it is a complicated integral) varied and caused beating of the spectum measurement. See Fig. 9(a). At present, the dispersion has been reduced, and the spectrum change with RF phase agrees closely with theory [Fig. 9(b)]. Thus, measurements of β distortions, anomalous dispersion, wakefield transverse tails and trajectory oscillation (generates dispersion) are needed independent of the spectrum measurement for a complete measurement to be performed.

EMITTANCE MEASUREMENT

The emittance of the beam along with the associated TWISS parameters can be measured in several ways: for example, by observing the change of the beam profile with changes in the strength of an upstream quadrupole or by observing the profile at three or more distinct locations in a betatron phase advance. An example of the quadrupole–profile monitor measurement is shown in Fig. 10. The measured ϵ, β, and α for Fig. 10 are $7.8\times10^{10}r-$m, 60 m, and -10, respectively. The effect of anomalous dispersion on the emittance measurements can be seen in Eq. (1). In order to extract $\epsilon, \beta, \alpha, \delta, \eta$ and η' from the measurements, six measurements are needed. An account of this process is given in Ref. 11. An example of an emittance measurement with multiple screens is discussed in the next section.

A summary of recent emittance measurements in the linac is given in Table 2. The effects considered in this paper are reflected in those results.

REAL TIME BEAM PROFILE MONITORING

The horizontal and vertical beam profiles of both positrons and electrons are measured in real time at full beam energy by deflecting the beams onto off-axis profile monitors at the rate of one pulse every two seconds.[12] A schematic view of this system is shown in Figs. 11 and 12. A dipole is excited on a single beam pulse deflecting positrons and electrons onto respective screens which are 5 mm from the accelerator axis. The profiles are digitized in x and y. Four combinations of dipole and profile monitor pairs were installed at 0, 22.5, 90 and 112.5 degrees in betatron phase. Only one combination is pulsed every two seconds allowing a complete measurement after eight seconds.

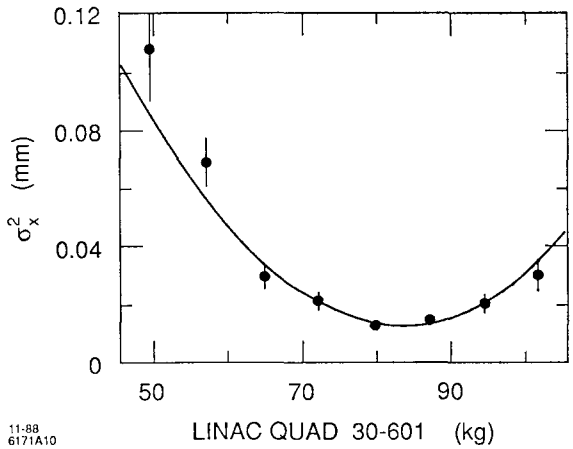

Fig. 10. Emittance measurement in the linac at 47 GeV showing the change in beam size with changes in the strength of an upstream quadrupole.

Table 2. Emittance of the SLC electron beam.

Location	$\gamma\epsilon_x$ (10^{-5} mrad)	$\gamma\epsilon_y$ (10^{-5} mrad)
Ext. Damping Ring	1.6	1.4
Ent. Linac	4.1	2.2
Ext. Linac	7.7	4.5
IP*	8.3	3.7

* corresponds to $\sigma_x = 5.3$ μm and $\sigma_y = 3.5$ μm for $\beta^* = 30$ mm.

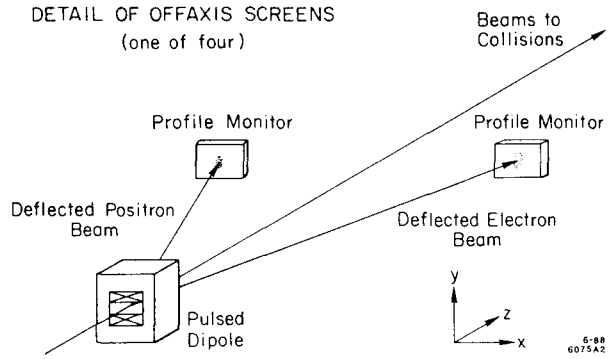

Fig. 12. Schematic of one of the four kicker-profile monitor combinations which allow both beams to be measured on a single linac pulse.

α_1 and γ_1 ($\beta_1\gamma_1 = 1+\alpha_1^2$) of the beam at the first profile monitor can be propagated to the other profile monitors using transport matrices. Let the transport matrix from the first monitor to the second be A_{ij} and the matrix from the first to the third be B_{ij}. The propagation of the TWISS parameters gives three equations for the measured beam sizes σ_1, σ_2, and σ_3:

$$\sigma_1^2 = \epsilon\beta_1$$

$$\sigma_2^2 = \epsilon\beta_2 = A_{11}^2\epsilon\beta_1 - 2A_{11}A_{12}\epsilon\alpha_1 + A_{12}^2\epsilon\gamma_1 \qquad (10)$$

$$\sigma_3^2 = \epsilon\beta_3 = B_{11}^2\epsilon\beta_1 - 2B_{11}B_{12}\epsilon\alpha_1 + B_{12}^2\epsilon\gamma_1 \quad .$$

There are three unknowns $\epsilon\beta_1, \epsilon\alpha_1$, and $\epsilon\gamma_1$, and three equations which can be solved by matrix inversion. The fourth measurement will be used for a consistency check. A computer history of these calculations is being implemented on the SLC control system.

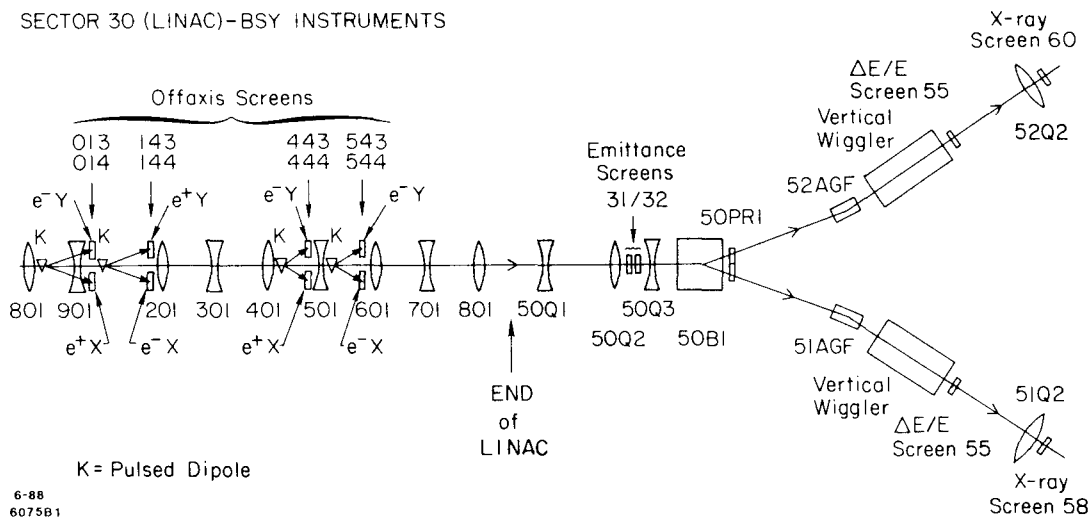

Fig. 11. Schematic layout of the instruments near the end of the linac. Pulsed dipoles (four) sequentially kick the e^+ and e^- beams onto off-axis profile monitors once every two seconds.

These images are viewed in the control room by the operators and are used to verify that the beam conditions have not changed. Examples of beam profiles are shown in Fig. 12. A normal profile combination is shown as well as ones which are distorted either by betatron mismatches or by anomalous dispersion.

An online emittance and TWISS parameter calculation can be performed with these measurements. The parameters ϵ, β_1,

CONCLUSIONS

During the commissioning phase of a new accelerator, beam dynamics verification absorbs a considerable fraction of the accelerator beam time. Therefore, it is important to have spent sufficient effort during the design stage of the project to provide systematic instrument packages to investigate beam dynamics. A reasonable amount of redundancy is important so

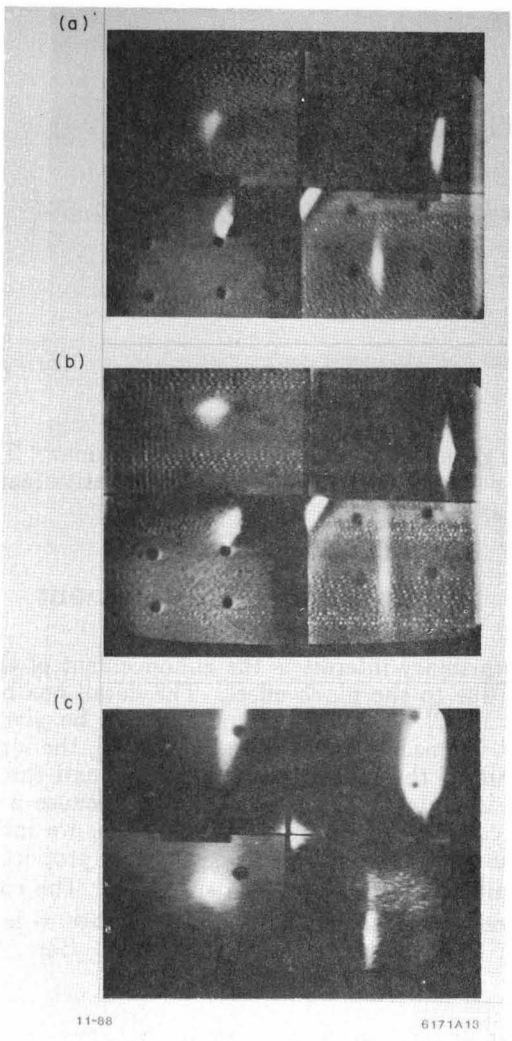

Fig. 13. Digitized "four" screen profile data for electrons using the equipment in Figs. 11 and 12. Photo (a) shows nominal beam profiles. Photo (b) shows enlargement of the beam due to betatron mismatches. Photo (c) shows enlargement of the beam due to a large anomalous dispersion in the linac.

that complimentary measurements can be used to resolve unexplained observations. These complimentary measurements often lead to the discovery of new phenomena either in beam dynamics or in the instrumentation. All accelerators have had effects which were not envisioned during their conception and construction. Finally, the various components of the accelerator complex should be tested as soon as possible during construction to get an advanced start on error correction.

ACKNOWLEDGEMENTS

The SLC was built and commissioned by many people from SLAC and associated universities. Many thanks are extended to the SLC Linac Group and the SLAC departments of Instrumentation and Control, Operations, Electronics, Mechanical Engineering, and Software for their contributions. Many thanks also go to M. L. Arnold and to the SLAC Publications Office for the preparation of this document.

REFERENCES

1. J. Sheppard, *Status of the SLC,* 1988 Linear Accelerator Conference, CEBAF, Williamsburg, VA.
2. J. Seeman and J. Sheppard, *Special SLC Linac Developments,* Stanford Linear Accelerator Conference, p. 214, 1986.
3. R. Erickson, Ed., *SLC Design Handbook,* SLAC Publication, December 1984.
4. T. Fieguth and J. Murray, *Design of the SLC Damping Ring to Linac Transport Lines,* 12th International Conference on High Energy Accelerators, FNAL, 1983.
5. J. Denard et al., *Monitoring of the Stanford Linac Microbunches' Position,* U. S. Particle Accelerator Conference, Santa Fe, 1983.
6. J. Seeman et al., *RF Beam Deflection Measurements and Corrections in the SLC Linac,* 1985 Particle Accelerator Conference, Vancouver, 1985, p. 2629.
7. M. Ross et al., *High Resolution Beam Profile Monitors in the SLC,* 1985 Particle Accelerator Conference, Vancouver, 1985.
8. K. Bane et al., *Bunch Lengthening in the SLC Damping Rings,* European Particle Accelerator Conference, Rome, 1988.
9. T. Himel, M. Lee, H. Shoaee, K. Thompson, private communication.
10. M. Ross, private communication.
11. J. Seeman and C. Adolphsen, *Beam Phase Space Determination at 50 GeV in the SLC Linac,* European Particle Accelerator Conference, Rome, 1988.
12. J. Seeman et al., *Transverse Wakefield Control and Feedback in the SLC Linac,* U. S. Particle Accelerator Conference, Washington, D.C., 1987.